Estimation of Power Losses Caused by Supraharmonics

Alexander Novitskiy[1,*], *Steffen Schlegel*[1], and *Dirk Westermann*[1]

[1]Technische Universität Ilmenau, Department of Electrical Engineering and Information Technology, 98693 Ilmenau, Germany

Abstract. Nowadays increases the number of power electronic devices in distribution electrical networks rapidly. Modern generation and consumption units use high switching frequency power converters for the network connection and therefore cause the voltage and current distortion in the frequency range over 2 kHz (so-called "supraharmonics") in addition to conventional harmonics. Supraharmonics cause additional power losses in electrical equipment. The goal of the offered paper is the estimation of power losses caused by supraharmonics. The estimation is based on the measurement results obtained in a real MV/LV network in Germany.

1 Introduction

The increase in the number of power electronic devices in distribution electrical networks is the characteristic trend in the development of electric power supply during many years. Modern generation and consumption units use high switching frequency power converters for the network connection and therefore cause the voltage and current distortion in the frequency range over 2 kHz (so-called "supraharmonics") in addition to conventional harmonics.

The presence of harmonic and supraharmonic distortion in electrical networks has a direct influence on the power and energy losses in the electrical equipment. The harmonic and supraharmonic currents cause the additional Joule heating of conductors and therefore increase the total power losses in these conductors.

The conductor resistance grows with the growth of the frequency and therefore relative small harmonic or supraharmonic currents can cause notable power losses.

In [1-3] is shown that additional power losses in LV cables and HV transmission lines caused by conventional current harmonics can be up to 30% regarding the power losses at the fundamental frequency.

The influence of supraharmonics on the additional power losses can be illustrated using the simplified assumption that the values of the line conductor resistances are proportional to the root of the frequency [2-5]:

$$R_{sh} = R_1 \sqrt{h} \qquad (1)$$

where R_{sh}, R_1 – resistance values at the supraharmonic frequency f_{sh} and at the fundamental frequency f_1 respectively, $h = f_{sh} / f_1$ is the harmonic order.

Using the calculation formula for the Joule heating and taking into account (1) the relative values of additional power losses caused by supraharmonics can be calculated as follows:

$$P_{Lsh} / P_{L1} = (I_{sh} / I_1)^2 \sqrt{h} \qquad (2)$$

where P_{Lsh}, P_{L1} – power losses caused by the supraharmonic current I_{sh} at the frequency f_{sh} and by the current I_1 at the fundamental frequency f_1 respectively.

The dependences (2) are presented in Fig. 1 for some ratios of I_{sh} / I_1.

It can be seen from Fig. 1 that additional power losses caused by a supraharmonic can be e.g. 10% and more regarding the power losses at the fundamental frequency and therefore cannot be neglected in the calculation of total power losses in electrical networks. The exact values of additional power losses are depending on the supraharmonic frequency and on the ratio I_{sh} / I_1.

It must be noted that (1) and (2) are valid mainly for overhead transmission lines.

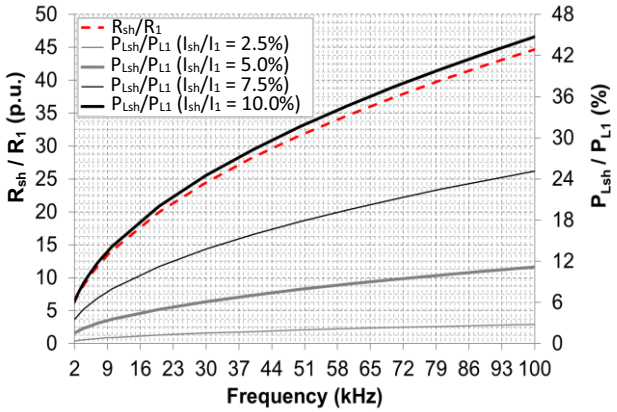

Fig. 1. Relative supraharmonic power losses (2) and the corresponding ratio R_{sh} / R_1

The estimation of power losses caused by supraharmonics in a cable feeder under real operating conditions is presented below. The estimation is based on the measurement results obtained in a real MV/LV network in Germany [6].

* Corresponding author: Alexander.Novitskiy@TU-Ilmenau.de

2 Measurements of supraharmonics

Results of the measurements carried out in the real MV/LV electrical network presented in Fig. 2 were used for the estimation of the impact of supraharmonics on the power losses in MV cable feeders.

The network supplies different settlments with mainly residential and commercial loads and contains a lot of decentralized renewable energy generating units. The network contains a MV wind plant and several solar parks (MV PV plants) distributed over the whole network and connected to the MV grid via dedicated transformers. Several powerful wind parks are located in the upstream HV network. Numerous LV PV power plants are connected in downstream LV distribution networks together with other power electronic devices using high switching frequency power converters like charging stations, consumer electronics, etc. via local area step-down MV/LV transformers.

Measurement devices SIRIUSi-HS [7] were located at the measuring points MP1 – MP3 and operated with the sampling rate 100 kHz. Supraharmonic voltage and current 200 Hz groups (according to [8, 9]) were recorded as 1 minute average values over the measuring interval of 2 weeks.

Power quality (PQ) parameters were measured at MP1 – MP3 in addition.

Instantaneous voltage values (sampling rate 10.240 kHz) and some PQ parameters as 1 sec average values were recorded at the measuring points W1-W24 (LV network) using measurement devices WeSense [10].

Influences of renewable energy sources on the supraharmonic distortion and the propagation of the supraharmonic distortion in the network under study were analysed in [6, 11, 12].

Power losses estimation in the supraharmonic frequency range can be done using the supraharmonic currents measured in the MV feeder at the distribution station. This is the measuring point MP2 (Fig. 2).

Measuring device at MP2 was connected to the secondary side of the instrument current transformer via current clamps. Current clamps were certified for the measurements in the frequency range up to 100 kHz.

The applicability of the standard MV instrument current transformer for the measurements in the supraharmonic frequency range was estimated taking into account IEC Technical Report 61869-103 [13] and investigation results [14, 15].

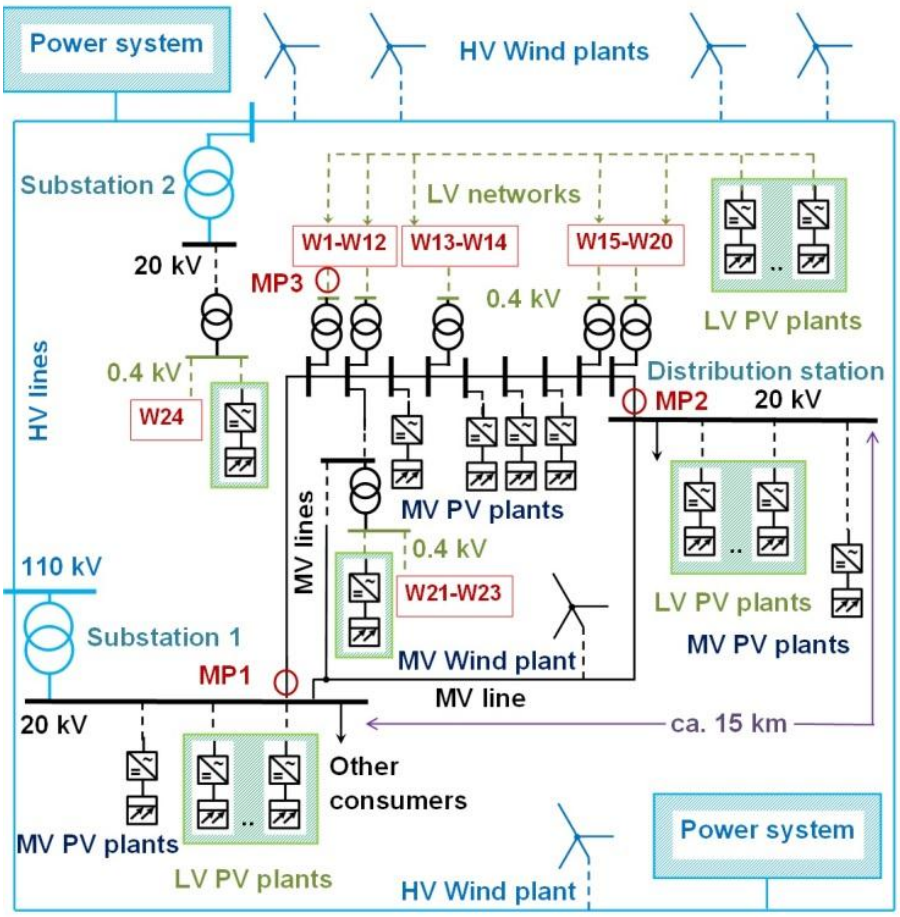

Fig. 2. MV/LV network under study and location of measuring devices

Supraharmonic frequency range is divided into a row of subranges. The supraharmonics in the frequency subrange up to 9 kHz are the subject of special consideration in the IEC standards for compatibility levels for conducted disturbances and signalling in public medium-voltage [16] and in low-voltage power supply systems [17]. Technical requirements for the connection and operation of customer installations to the MV network in Germany contains admissible values for the supraharmonic currents in the frequency range 2 to 9 kHz [18]. Therefore is necessary to pay special attention to the transfer characteristics of MV instrument current transformers in the frequency range 2 to 9 kHz.

In [13] is noted that inductive current transformers are suitable for the use in the supraharmonic frequency range 2 to 9 kHz. Taking into consideration the measured frequency dependences for ratio and phase errors of MV instrument current transformers presented in [14] and [15] it can be concluded that the supraharmonic currents can be measured using standard MV instrument current transformers with a sufficient accuracy (amplitude errors up to a few percent) for the simplified estimation of power losses in the frequency range 2 to 9 kHz.

Examples of measured current spectra in the MV feeder (MV distribution station, measuring point MP2) are presented in Fig. 3 and 4.

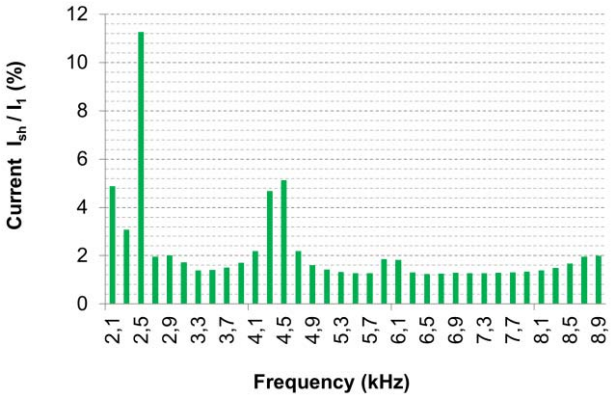

Fig. 3. Measured current spectrum, 95% quantiles of 1 min average values, 200 Hz groups, measurement time 24 h, MP2

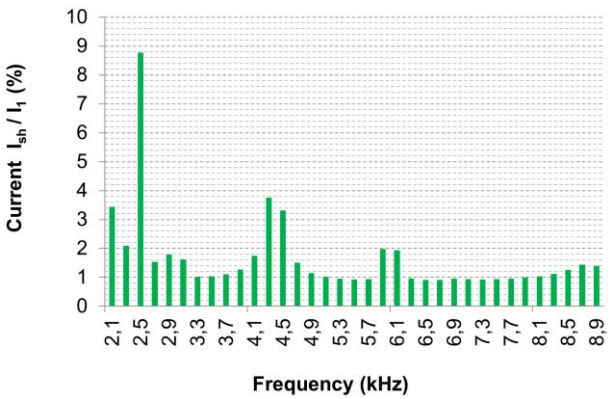

Fig. 4. Measured current spectrum, 95% quantiles of 1 min average values, 200 Hz groups, measurement time one week, MP2

It can be seen from Fig. 3 and 4 that the current spectra are characterized by the domination of the supraharmonic component 2.5 kHz. In [6, 12] is shown that the components 2.5 kHz in the network under study are mainly caused by the operation of the MV wind plant.

The components 5.9 and 6.1 kHz are caused by the daily operation of solar plants, the components 4.3 and 4.5 kHz are caused by the changes of operating points of connected units.

The measuring point MP2 is the connection point of the MV cable 3x1x150/25 to the busbar of the distribution station. This MV cable connection contains three single-core cables with aluminium conductors of 150 mm^2 and copper screens of 25 mm^2 for each cable.

Determination of the frequency dependences for the cable resistances is considered below.

3 Determination of the frequency dependences for the cable resistances

3.1. Analytic calculation method

Calculation of AC resistance of conductor is a part of the IEC standard [19]. In [19] is noted that the AC cable conductor resistance is depending on the skin and on the proximity effects. The following formula can be used:

$$R_{sh} = R'_{DC} (1+Y_S+Y_P) \quad (3)$$

where R_{sh} –conductor resistance at the supraharmonic frequency f_{sh}, R'_{DC} – DC resistance of conductor at the maximum operating temperature θ, Y_S – skin effect factor, Y_P – proximity effect factor.
The values of Y_S and Y_P are depending on the values of the factors X_S and X_P as follows:

$$X^2_S = (1 / R'_{DC}) \, 8\pi f_{sh} \, 10^{-7} \, k_S \quad (4)$$

and

$$X^2_P = (1 / R'_{DC}) \, 8\pi f_{sh} \, 10^{-7} \, k_P \quad (5)$$

where k_S, k_P – coefficients, e.g. $k_S = 1$ and $k_P = 1$ for cables with copper or aluminium solid conductors[19].
The skin effect factor Y_S is given by the following equations [19]:

For $0 < X_S \leq 2.8$

$$Y_S = (X^4_S / 192 + 0.8 \, X^4_S) \quad (6)$$

For $2.8 < X_S \leq 3.8$

$$Y_S = -0.136 - 0.0177 \, X_S + 0.056 \, X^2_S \quad (7)$$

For $3.8 < X_S$

$$Y_S = 0.354 \, X_S - 0.733 \quad (8)$$

The proximity effect factor Y_P according to [19] can be calculated only if the factor X_P does not exceed 2.8.

It can be seen from (4) and (5) that $X_P = X_S$ for the cables with solid conductors taking into consideration the assumption $k_S = k_P = 1$ [19].

The values of X_P and X_S calculated according to (4) and (5) for the cables with solid aluminium conductors are presented in Fig. 5 and 6. The values R'_{DC} in (4) and (5) were determined for each cross-sectional area according to [20] taking into account the standard formula [19]:

$$R'_{DC} = R_{DC} [1+\alpha_{20} (\theta-20)] \quad (9)$$

where R_{DC} – DC resistance of conductor at 20°C, R'_{DC} – DC resistance of conductor at the maximum operating temperature θ, α_{20} is the constant mass temperature coefficient at 20°C per Kelvin.

The calculation results for the operating temperature 20°C are presented in Fig. 5, the calculation results for the maximum operating temperature 90°C are presented in Fig. 6.

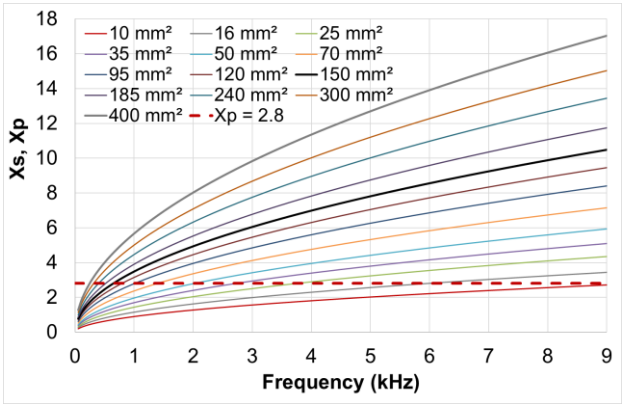

Fig. 5. Factors X_S and X_P for cable aluminium solid conductors at the operating temperature 20°C

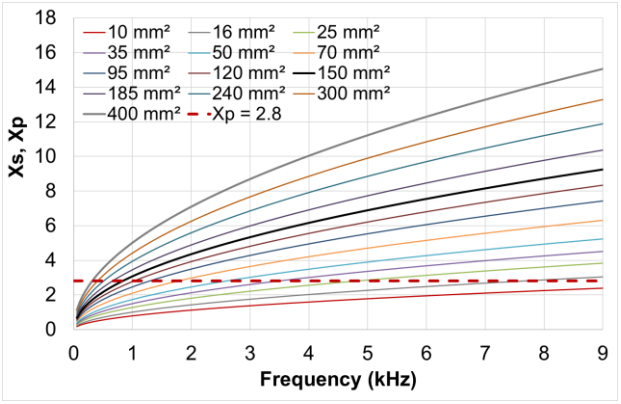

Fig. 6. Factors X_S and X_P for cable aluminium solid conductors at the operating temperature 90°C

It can be clearly seen from Fig. 5 and 6 that the cable aluminium solid conductors with the standard cross-sectional areas starting from 16 mm^2 and larger are characterized by the values of X_P higher than 2.8 at least at some frequencies in the frequency range 2 to 9 kHz.

Cable aluminium solid conductors with the standard cross-sections of 70 mm^2 and larger are characterized by the values of X_P higher than 2.8 in the full frequency range 2 to 9 kHz.

It means that the method for the analytic calculation of frequency-dependent cable resistances [19] is not applicable to the calculation of resistances at supraharmonic frequencies in many practical cases due to the constraints on the combination of parameters considered in [19].

More common analytic method for the calculation of frequency-dependent cable resistances is published in [21].

The analytic method for the calculation of the skin effect factor Y_S in [21] is identical with the method [19] described above.

The following formula is suggested in [21] for the calculation of the proximity effect factor Y_P for three single-core cables:

$$Y_P = m\, y^2\, G_P /(2 - 5\, y^2\, H_P /12) \quad (10)$$

where m = 3 for three single-core circular cables, y – spacing ratio, G_P, H_P – coefficients.
The coefficients G_P, H_P are given by the following equations [21]:

For $0 < X_P \le 2.8$

$$G_P = 11\, X^4_P / (704 + 20\, X^4_P) \quad (11)$$

For $2.8 < X_P \le 3.8$

$$G_P = -0.08\, X^2_P + 0.72\, X_P - 1.04 \quad (12)$$

For $3.8 < X_P$

$$G_P = X_P / (4\sqrt{2}) - 1/8 \quad (13)$$

For $0 < X_P \le 2.8$

$$H_P = (1/3)\,(1 + 0.0283\, X^4_P) / (1 + 0.0042\, X^4_P) \quad (14)$$

For $2.8 < X_P \le 3.8$

$$H_P = 0.0384\, X^2_P + 0.119\, X_P + 0.095 \quad (15)$$

For $3.8 < X_P$

$$H_P = (2X_P - 4.69) / (X_P - 1.16) \quad (16)$$

The spacing ratio $y = d_c / s$, where s is the spacing between conductor axes, d_c is the diameter of an equivalent circular conductor.

The construction of the MV cable 3x1x150/25 means that each cable conductor is surrounded by a cable screen.

The AC currents flowing in the cable conductors cause the induced currents in the surrounding cable screens and therefore cause some additional power losses in the screens. It means the increase of equivalent cable resistances at the frequencies of the AC currents

(fundamental frequency, harmonic and supraharmonic frequencies).

Therefore the formula (3) can be extended to consider the influence of the power losses in the cable screens on the conductor resistance as follows:

$$R_{sh} = R'_{DC} (1+Y_S+Y_P+Y_{SC}) \quad (17)$$

where Y_{SC} – the screen losses factor.

It must be noted that each cable containing axial conductor surrounded by a cable screen can be considered as a pipe-type cable. Taking into account the relation given in [22] for the consideration of the increase in losses in the phase conductors due to the proximity of the pipe the following formula can be used for the screen losses factor:

$$Y_{SC} = 0.5 (Y_S+Y_P) \quad (18)$$

These considerations are in compliance with the recommendation [19] for the calculation of AC cable conductor resistances for pipe-type cables. The following formula can be used according to [19]:

$$R_{sh} = R'_{DC} [1+1.5(Y_S+Y_P)] \quad (19)$$

Using (4) – (16), (19) the values of the conductor resistances at the supraharmonic frequencies R_{sh} and the relations R_{sh} / R_1 can be analytic determined for the MV cable 3x1x150/25 under study.

3.2 Numerical calculation method

The use of the finite element method (FEM) is a popular approach for the numerical calculation of the frequency dependences for the cable resistances.

The advantages of this method are the exact modelling of the cable geometry, the simulation of the properties of the materials used in the cable construction and the simultaneous consideration of all influencing effects named above: the skin effect, the proximity effect, the influence of the cable screens and all other metallic elements (e.g. cable armour, pipes, ducts, trays, etc.) which can have an influence on the AC resistances of the cable conductors.

Using the FEM approach it is possible to calculate the current density distribution in all parts of the simulated cable construction. Taking into account the cable geometry and the electrical conductivities of simulated constructive materials the power losses in all elements of the cable construction can be determined.

The calculation of the equivalent AC resistance of the cable conductor R_{sh} at the supraharmonic frequency f_{sh} can be carry out taking into consideration the following formula:

$$P_{Lsh} = I^2_{sh} R_{sh} \quad (20)$$

where P_{Lsh} – the average value of total power losses caused by the simulated supraharmonic conductor current I_{sh} at the frequency f_{sh} in each phase of the three-phase cable system.

In respect to the considered MV cable construction 3x1x150/25:

$$P_{Lsh} = P_{Lsh\ cond} + P_{Lsh\ sc} \quad (21)$$

where $P_{Lsh\ cond}$ – the average value of the power losses in each phase conductor and $P_{Lsh\ sc}$ – the average value of the power losses in each conductor screen.

For the determination of the frequency dependence for the equivalent AC cable resistance it is necessary to carry out the row of the simulations at different frequencies. The frequency dependence can be determined from the following relations:

$$P_{Lsh} / P_{L1} = I^2_{sh} R_{sh} / I^2_1 R_1 \quad (22)$$

The values I_{sh} and I_1 can be taken e.g. from the measurement results.

Taking into account the FEM simulation of the heating processes the cable operating temperature can be determined and the influence of the temperature on the electrical conductivity can be considered additionally [23-25].

For the simplification of the calculations it is enough to assume $I_{sh} = I_1$. In this case is enough to calculate the power losses (21) for each frequency under consideration. The formula (22) will be simplified as follows:

$$P_{Lsh} / P_{L1} = R_{sh} / R_1 \quad (23)$$

Using (23) the frequency dependence for the equivalent AC cable resistance can be determined.

It must be noted that the electrical conductivity of the cable insulation is very small in comparison with the conductivities of the cable conductors and metallic screens. Therefore it is enough to simulate only metallic parts of the cable configuration to simplified estimate the power losses (20) and to calculate the equivalent AC resistance of the cable conductor.

Fig. 7 presents a simulation example for the MV cable 3x1x150/25. The trefoil formation with the spacing between conductor axes of 40 mm was simulated. Both aluminium conductors and copper screens were simplified represented as solid objects.

The simulation was carried out using the software package FEMM [26].

The calculated current density distribution J in the aluminium cable conductors and in the copper cable screens is shown in Fig. 7. The supraharmonic phase conductor currents of I_{sh} = 0.54 A (r.m.s. value) at the frequency f_{sh} = 2.5 kHz were simulated as the origin of the magnetic field in the cable. This value of the conductor current was measured as 1 min value during the measurement campaign at the measuring point MP2.

The conductor currents were simulated as a three-phase set of balanced phasors with the difference of phase angles of 120° between two neighboring phasors.

Fig. 8 presents the line plot of the current density for the straight line contour crossing the centers of two neighboring conductors with screens. The coordinates of centers in the "position" axis are - 20 mm and + 20 mm respectively. The skin effect, the proximity effect, the influence of the cable screens can be clearly seen from Fig. 8.

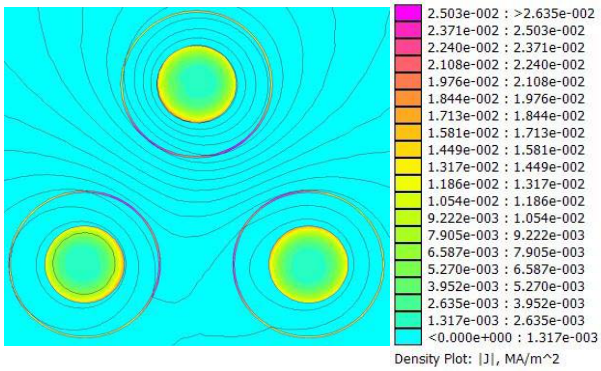

Fig. 7. Current density distribution J in the aluminium conductors and copper screens of the MV cable 3x1x150/25 caused by the supraharmonic current 0.54 A (r.m.s. value) at the frequency 2.5 kHz

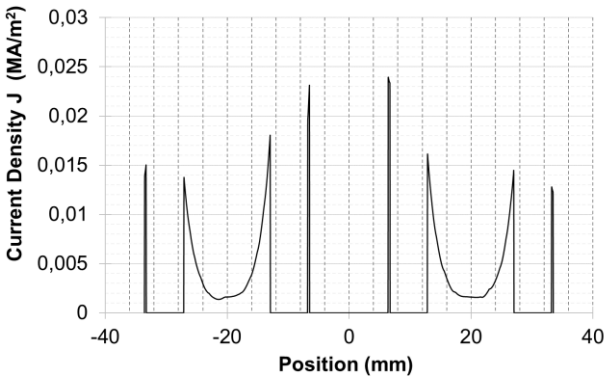

Fig. 8. Current density distribution J along the straight line crossing the centers of two neighboring conductors and screens of the MV cable 3x1x150/25 caused by the supraharmonic current 0.54 A (r.m.s. value) at the frequency 2.5 kHz

3.3 Calculated frequency dependences for the MV cable under study

The analytic calculated frequency dependences R_{sh} / R_1 for the MV cable 3x1x150/25 are presented in Fig. 9. It is the frequency dependence calculated taking into account only the skin effect (parameter Y_S), the frequency dependence calculated taking into account both the skin and the proximity effects (parameters Y_S and Y_P), the frequency dependence calculated taking into account the skin effect, the proximity effect and the influence of the power losses in the conductor screens (parameters Y_S, Y_P, Y_{SC}).

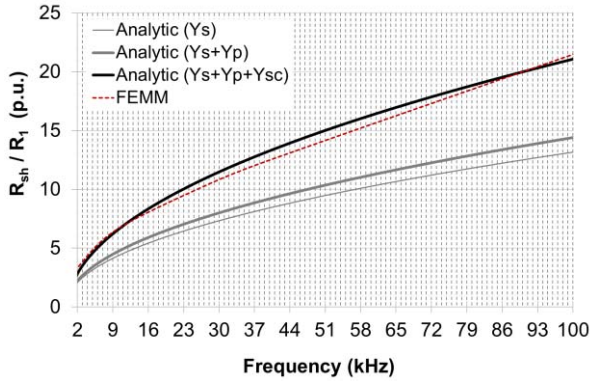

Fig. 9. Analytic and numerical (with the use of FEMM software) determined frequency dependences R_{sh}/R_1 for the MV cable 3x1x150/25 in the supraharmonic frequency range

The frequency dependence R_{sh} / R_1 determined with the use of the software package FEMM for numerical calculations is presented in Fig. 9 for the comparison.

The corresponding reference values R_{sh} / R_1 = 1 were calculated for each presented dependence taking into consideration the fundamental frequency 50 Hz.

It can be seen from Fig. 9 that the skin effect is the dominating factor in the increase of the equivalent AC resistance of the cable conductor R_{sh} with the increase of the frequency in the supraharmonic frequency range.

It can be seen from Fig. 9 that the influence of the power losses in the conductor screens on the increase of the equivalent AC resistance of the cable conductor R_{sh} with the increase of the frequency is much higher in comparison with the influence of the proximity effect for the MV cable under study.

It can be concluded from the comparison of the analytic and numerical calculated frequency dependences presented in Fig. 9 that the analytic formula (17) parametrized according to (18) or the direct formula (19) are most suitable for the analytic characterization of the increase of the equivalent AC resistance of the cable conductor R_{sh} with the increase of the frequency for the MV cable under study in the supraharmonic frequency range 2 to 100 kHz.

Taking into consideration the frequency dependence (1) presented graphically in Fig. 1 it can be concluded that the frequency dependences calculated by (19) or using FEM simulations for the MV cable under study are characterized by lower values of the relations R_{sh} / R_1 than the square root from the harmonic order $h = f_{sh} / f_1$.

For the supraharmonic frequency range 2 to 9 kHz the following formula can be suggested for the simplified representation of the frequency dependence of R_{sh} / R_1 for the MV cable under study:

$$R_{sh} / R_1 \approx 0.48 \sqrt{h} \qquad (24)$$

Deviations of (24) from the FEMM calculation results do not exceed a few percent in the range 2 to 9 kHz.

4 Use of measurement results for the supraharmonic power losses estimation

Using (22) the supraharmonic power losses in the MV cable under study can be determined. For clarity (22) can be represented similar to (2) and rewritten as follows:

$$P_{Lsh} / P_{L1} = (I_{sh} / I_1)^2 R_{sh} / R_1 \quad (25)$$

Taking into consideration calculated frequency dependences R_{sh} / R_1 for the MV cable under study and the measurement results for the time rows I_{sh} / I_1 obtained during the measurement campaign the time rows for the relative values of supraharmonic power losses P_{Lsh} / P_{L1} can be determined.

Fig. 10 and 11 show the supraharmonic spectrums of relative power losses in the frequency range 2 to 9 kHz in the 20 kV cable feeder under study determined according to (25) for the measurement interval of 24 h (Fig. 10) and for the measurement interval of one week (Fig. 11).

The spectrums in Fig.10 and 11 are presented for the supraharmonic groups of 200 Hz in accordance with the obtained measurement results for the supraharmonic currents. For the center frequencies of each group the frequency dependences R_{sh} / R_1 calculated according to (19) were taken into consideration.

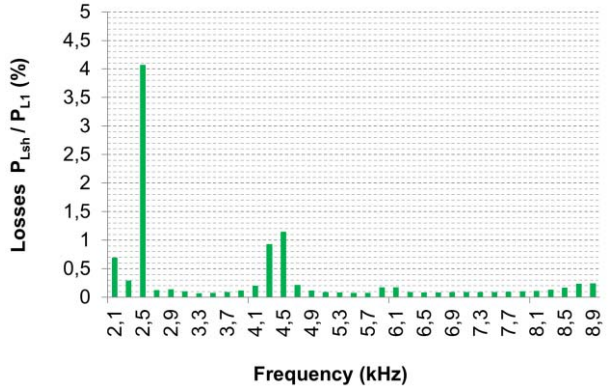

Fig. 10. Relative power losses in a 20 kV cable feeder, 95% quantiles of 1 min values, 200 Hz groups, measurement time 24 h, MP2

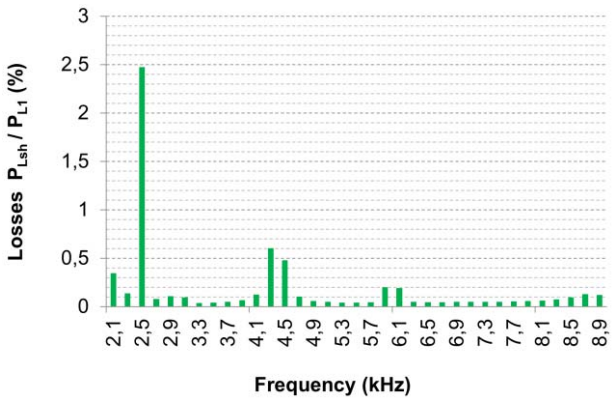

Fig. 11. Relative power losses in a 20 kV cable feeder, 95% quantiles of 1 min values, 200 Hz groups, measurement time one week, MP2

It must be noted that the sum of average values of 1 min relative harmonic power losses (harmonics 2nd to 40th) for this measurement day considered in Fig. 10 is 24.4%, the sum of average values of 1 min relative supraharmonic power losses in the range 2 to 9 kHz presented in Fig. 10 is 2.4%. The sum of average values of 1 min relative harmonic power losses for the complete measurement week considered in Fig. 11 is 12.9%, the sum of average values of 1 min relative supraharmonic power losses in the range 2 to 9 kHz presented in Fig. 11 is 1.6%.

It means that the supraharmonic power losses are present in modern distribution networks and can reach the values of several percent with respect to the power losses at the fundamental frequency. The results of the analysis show that supraharmonic power losses can exceed 10% regarding the power losses caused by conventional current harmonics in the MV cable under study. Therefore it can be recommended to consider supraharmonic power losses for a correct estimation of total power losses in modern distribution networks.

5 Summary

Method of the supraharmonic power losses estimation combining the analytic determination of AC cable resistances at the supraharmonic frequencies with the use of measurement results of supraharmonic currents in a real MV/LV cable network was considered in the paper.

Analytic calculation results of the determination of AC cable resistances at the supraharmonic frequencies were verified and precisized using the FEM simulations for a MV cable chosen for the investigation. A simplified formula for the estimation of the increase of the AC cable resistances with respect to the cable resistance at the fundamental frequency of the MV cable under study for the frequency range 2 to 9 kHz was suggested.

It was noted that supraharmonic power losses in MV networks in the frequency range 2 to 9 kHz can be simplified estimated using the measurement results obtained by conventional current measuring instruments.

It was shown that supraharmonic power losses in the MV cable under study operating in a real network can reach the values of several percent with respect to the power losses at the fundamental frequency and can exceed 10% regarding the power losses caused by conventional current harmonics.

It can be recommended to consider supraharmonic power losses for a correct estimation of total power losses in networks with high presence of power electronics.

References

1. L. Topolski, J. Warecki, Z. Hanzelka, Calculating Power Losses In LV Cables Loaded With Nonsinusoidal Currents, *Proc. of the conf.*

Computational Problems of Electrical Engineering (CPEE), 9-12 Sept. 2018, Banska Stiavnica, Slovakia (2018)

2. N. Kharlov, V. Borovikov, V. Litvak, A. Pogonin, V. Melnikov. Energy survey of non-sinusoidal operating states of multiconductor power transmission lines. "Electrichestvo (Electricity)" № **12**, pp 12-15 (2011) (in Russian)
3. N. Kharlov, V. Borovikov. Results of a survey of operating states of distribution electrical networks of Siberia and southern Russia. *Proc. of the conf. Energy-21: Sustainable Development & Smart Management*, Sept. 1-3, 2015, Irkutsk, Russia (2015) (in Russian)
4. J. Zhu, E. Bećirović, J. Milanović. The Effect of Network Modelling on Harmonic Propagation Studies in Power Electronics Rich Transmission Networks. *Proc. of the conf. IET International Conference on Advances in Power System Control, Operation and Management (APSCOM 2018)*, Nov. 11-15, Hong Kong, China (2018)
5. T.A. Short. *Electric Power Distribution Equipment and Systems*. CRC Press (2006)
6. A. Novitskiy, S. Schlegel, D. Westermann, Measurements and Analysis of Supraharmonic Influences in a MV/LV Network Containing Renewable Energy Sources, *Proc. of Electric Power Quality and Supply Reliability Conference (PQ) & Symposium on Electrical Engineering and Mechatronics (SEEM)*, Kärdla, Estonia, 2019, pp. 1-6 (2019)
7. *SIRIUS® Technical Reference Manual*. DEWESoft (2015)
8. Electromagnetic compatibility (EMC) – Part 4-7: Testing andmeasurement techniques – General guide on harmonics and interharmonics measurements and instrumentation, for power supply systems and equipment connected thereto, IEC 61000-4-7 (2009)
9. Electromagnetic compatibility (EMC) – Part 4-30: Testing and measurement techniques – Power quality measurement methods, IEC 61000-4-30 (2015)
10. C. Rüster, F. Haussel, T. Hühn, N. El Sayed, VEREDELE-FACDS Field Trial: Wide Area Power Quality Assessment With IOT Sensors and Cloud-Based Analytics, *Proc. of Int. ETG Congress 2017*, Nov. 28-29, 2017, Bonn, Germany (2017)
11. A. Novitskiy, S. Schlegel, D. Westermann. Analysis of Supraharmonic Propagation in a MV Electrical Network, *Proc. of 19th Int. Sc. Conf. EPE 2018*, May 16-18, 2018, Brno, Czech Republic (2018)
12. A. Novitskiy, P. Tikhonov, T. Jiang, S. Schlegel, T. Hühn, N. El Sayed, C. Rüster, D. Westermann. Influence of Renewable Energy Sources on Supraharmonic Distortion in Modern MV/LV Distribution Networks. *Proc. of the Int. Conf. Power Quality Management (PQM)*, Dec. 5-7, 2018, Moscow, Russia (2018)
13. Instrument Transformers - The use of instrument transformers for power quality measurement, IEC/TR 61869-103 (2012)
14. K. Kunde, H. Däumling, R. Huth, H.-W. Schlierf, J. Schmid. Frequency Response of Instrument Transformers in the kHz range. etz, Heft **6**/2012, pp. 1-4 (2012)
15. M. Redfern, S. Terry, F. Robinson, Z. Bo. A Laboratory Investigation into the use of MV Current Transformers for Transient Based Protection. *Proc. of Int. Conf. on Power Systems Transients – IPST 2003*, Sept. 28-Oct. 2, 2003, New Orleans, USA (2003)
16. Electromagnetic compatibility (EMC) — Part 2-12: Environment — Compatibility levels for low-frequency conducted disturbances and signalling in public medium-voltage power supply systems. IEC 61000-2-12 (2003)
17. Electromagnetic compatibility (EMC) — Part 2-2: Environment — Compatibility levels for low-frequency conducted disturbances and signalling in public low-voltage power supply systems. IEC 61000-2-2 (2018)
18. VDE-AR-N-4110. Technical Requirements for the connection and operation of customer installations to the medium voltage network (TAR medium voltage), Technische Regeln für den Anschluss von Kundenanlagen an das Mittelspannungsnetz (TAR Mittelspannung), Nov. 2018 (2018) (in German)
19. IEC 60287-1-1. Electric cables – Calculation of the current rating – Part 1-1: Current rating equations (100 % load factor) and calculation of losses – General. Ed. 2.1 (2014)
20. IEC 60228. Conductors of insulated cables. Ed.3.0 (2004)
21. Y. Du and J. Burnett, Experimental Investigation into Harmonic Impedance of Low-Voltage Cables, IEE Proceedings - Generation, Transmission and Distribution, Vol. **147**, Issue 6, Dec. 2000, pp. 322-328 (2000)
22. J. Palmer, R. Degeneff, T. McKernan, T. Halleran. Pipe-Type Cable Ampacities in the Presence of Harmonics. IEEE Transactions on Power Delivery, Vol. **8**. No. 4, October 1993, pp. 1689-1695 (1993)
23. W. Frelin, L. Berthet, Y. Brument, M. Petit, G. Perujo, J. Vannier. Thermal Behavior of LV Cables in Presence of Harmonic Currents. *Proc, of XIV Int. Symp. on Electromagnetic Fields in Mechatronics, Electrical and Electronic Engineering ISEF 2009*, Sept. 10-12, 2009, Arras, France, (2009)
24. S. Dubitsky, G. Greshnyakov, N. Korovkin. Refinement of Underground Power Cable Ampacity by Multiphysics FEA Simulation. Int. Journal of Energy, Vol. **9**, 2015, pp. 12-19 (2015)
25. Electric Cables—Calculations for Current Ratings—Finite Element Method, IEC/TR 62095 (2003)
26. D. Meeker. *Finite Element Method Magnetics*, User's Manual, Ver. 4.2 (2018)